MAXI GSC monitoring of the Crab nebula and pulsar during the GeV gamma-ray flare in September 2010

Mikio Morii,[1] Mutsumi Sugizaki,[2] Nobuyuki Kawai,[1] Motoko Serino,[2] Takayuki Yamamoto,[2, 3] Ryuichi Usui,[1] Arata Daikyuji,[4] Ken Ebisawa,[5] Satoshi Eguchi,[6] Kazuo Hiroi,[6] Masaki Ishikawa,[7] Naoki Isobe,[6] Kazuyoshi Kawasaki,[8] Masashi Kimura,[9] Hiroki Kitayama,[9] Mitsuhiro Kohama,[8] Takanori Matsumura,[10] Masaru Matsuoka,[2] Tatehiro Mihara,[2] Yujin E. Nakagawa,[11] Satoshi Nakahira,[12] Motoki Nakajima,[13] Hitoshi Negoro,[3] Hiroshi Ozawa,[3] Megumi Shidatsu,[6] Tetsuya Sootome,[2] Kousuke Sugimori,[1] Fumitoshi Suwa,[3] Hiroshi Tomida,[8] Yohko Tsuboi,[10] Hiroshi Tsunemi,[9] Yoshihiro Ueda,[6] Shiro Ueno,[8] Akiko Uzawa,[10] Kazutaka Yamaoka,[12] Kyohei Yamazaki,[10] and Atsumasa Yoshida[12]

[1] *Department of Physics, Tokyo Institute of Technology, Ookayama 2-12-1, Meguro-ku, Tokyo 152-8551, Japan*
morii@hp.phys.titech.ac.jp

[2] *Coordinated Space Observation and Experiment Research Group, Institute of Physical and Chemical Research (RIKEN), 2-1 Hirosawa, Wako, Saitama 351-0198, Japan*

[3] *Department of Physics, Nihon University, 1-8-14 Surugadai, Chiyoda, Tokyo 101-8308, Japan*

[4] *Department of Applied Physics, University of Miyazaki, 1-1 Gakuen Kibanadai-nishi, Miyazaki, Miyazaki 889-2192, Japan*

[5] *Department of Space Science Information Analysis, Institute of Space and Astronautical Science, Japan Aerospace Exploration Agency, 3-1-1 Yoshino-dai, Chuo-ku, Sagamihara, Kanagawa 252-5210, Japan*

[6] *Department of Astronomy, Kyoto University, Oiwake-cho, Sakyo-ku, Kyoto 606-8502, Japan*

[7] *School of Physical Science, Space and Astronautical Science, The graduate University for Advanced Studies (Sokendai), Yoshinodai 3-1-1, Chuo-ku, Sagamihara, Kanagawa 252-5210, Japan*

[8] *ISS Science Project Office, Institute of Space and Astronautical Science, Japan Aerospace Exploration Agency, 2-1-1 Sengen, Tsukuba, Ibaraki 305-8505, Japan*

[9] *Department of Earth and Space Science, Osaka University, 1-1 Machikaneyama, Toyonaka, Osaka 560-0043, Japan*

[10] *Department of Physics, Faculty of Science and Engineering, Chuo University, 1-13-27 Kasuga, Bunkyo-ku, Tokyo 112-8551, Japan*

[11] *High Energy Astrophysics Laboratory, Institute of Physical and Chemical Research (RIKEN), 2-1 Hirosawa, Wako, Saitama 351-0198, Japan*

[12] *Department of Physics and Mathematics, Aoyama Gakuin University, 5-10-1 Fuchinobe, Chuo-ku, Sagamihara, Kanagawa 252-5258, Japan*

[13] *School of Dentistry at Matsudo, Nihon University, 2-870-1 Sakaecho-nishi, Matsudo, Chiba 271-8587, Japan*

(Received 2011 April 19; accepted 2011 July 20)

Abstract

We report on the MAXI GSC X-ray monitoring of the Crab nebula and pulsar during the GeV gamma-ray flare for the period of 2010 September 18−24 (MJD 55457−55463) detected by AGILE and Fermi-LAT. There were no significant variations on the pulse phase averaged and pulsed fluxes during the gamma-ray flare on time scales from 0.5 to 5 days. The pulse profile also showed no significant change during this period. The upper limits on the variations of the pulse phase averaged and pulsed fluxes for the period MJD 55457.5−55462.5 in the 4−10 keV band are derived to be 1 and 19%, respectively, at the 90% confidence limit of the statistical uncertainty. The lack of variations in the pulsed component over the multi-wavelength range (radio, X-ray, hard X-ray, and gamma-ray) supports not the pulsar but the nebular origin for the gamma-ray flare.

Key words: stars: neutron — stars: pulsars: individual (Crab) — X-rays: individual (Crab)

1. Introduction

The Crab nebula has been the standard candle in high energy X-ray and gamma-ray astronomy. The flux and spectrum in these energy ranges have been expected to be steady over years. Surprisingly, AGILE and Fermi-LAT reported a flare for the period of 2010 September 18−24 in the GeV gamma-ray energy range (Tavani et al. 2010; Buehler et al. 2010; Tavani et al. 2011; Abdo et al. 2011). The first half of the flare (September 18−21) was detected by both AGILE and Fermi-LAT, while that of the second half (September 21−24) was detected only by Fermi-LAT. The half-day binned light curve of Fermi-LAT exhibited three sub-flares during these periods (Balbo et al. 2011).

INTEGRAL observed the Crab nebula from 10:32 on September 12 to 12:48 on September 19 (UT) for calibration purposes, which covered the first fifth of the gamma-ray flare. It detected no significant flux increase in the 20−400 keV range (Ferrigno et al. 2010a). Swift BAT detected no variations over the uncertainty of 5.5% at the 1-σ limit in the 15−50 keV range for the period of 2010 September 19−21 (Markwardt, Barthelmy & Baumgartner 2010). Radio observations of the Crab pulsar showed no evidence of a pulsar glitch and also no change on the pulsed flux as well as the pulse profile (Espinoza et al. 2010). ARGO-YBJ reported an excess of events (4 σ) from a direction consistent with the Crab nebula, corresponding to a flux about 3−4 times higher than usual, at the median energy of about 1 TeV (Aielli et al. 2010). On the other hand, MAGIC and VERITAS reported no significant enhancement in the TeV gamma-ray flux during the GeV flare (Mariotti et al. 2010; Ong et al. 2010). The

Swift XRT follow-up observation of 1-ks exposure starting on September 22 at 16:42 (UT), which corresponds to the third sub-flare recognized in the Fermi-LAT light curve (Balbo et al. 2011), showed no changes of flux, spectrum or pulse profile (Evangelista et al. 2010). Swift XRT detected no active AGN near the Crab nebula (Heinke 2010). The INTEGRAL follow-up observation from 21:05 on September 22 to 11:12 on September 23 (UT), approximately corresponding to the end of the flare, found no significant change in the pulse profile in the 20−40 keV band (Balbo et al. 2011).

After the gamma-ray flare, the RXTE PCA follow-up observation on September 24 showed no changes of flux, spectrum nor pulse profile (Shaposhnikov et al. 2010). The follow-up observation in a near-infrared wavelength on September 24 showed no variation in the Crab pulsar in the J and H bands (Kanbach et al. 2010). The follow-up observations by Chandra on September 28 and the HST on October 2 revealed an anvil feature close to the base of the pulsar jet and elongated striation at the distant place (Tennant et al. 2010; Ferrigno et al. 2010b; Horns et al. 2010; Tavani et al. 2011). These features are thought to indicate a particle acceleration and the origin of the GeV gamma-ray flare (Tavani et al. 2011). Two further GeV gamma-ray flare episodes, detected by AGILE on 2007 October and by Fermi-LAT on 2009 February, were reported (Tavani et al. 2011; Abdo et al. 2011). None of these three gamma-ray flares showed any changes of the pulsed component in the GeV energy range.

Another surprising thing is the long-term variability of the Crab nebula in the hard X-ray bands reported by Wilson-Hodge et al. (2011). The total nebula flux was found to decrease from 2008 August to 2010 July and the fractional decline was larger in higher energy ranges. On the other hand, the pulsed flux in the $3.2-35$ keV band of RXTE PCA decreased steadily at $\sim 0.2\%$ yr^{-1}, consistent with the pulsar spin-down, indicating that the observed X-ray variability would originate not from the pulsar but from the nebula.

MAXI has been monitoring the Crab nebula since the beginning of the mission on 2009 August 15 (UT), which covered the whole gamma-ray flare in 2010 September. Here, we report on the MAXI monitoring of the pulse phase averaged and pulsed fluxes of the Crab nebula, as well as the pulse profile.

2. Observation

MAXI (Monitor of All-sky X-ray Image) is an X-ray all-sky monitor, mounted on the Japanese Experiment Module - Exposed Facility of the International Space Station (Matsuoka et al. 2009). It carries two types of X-ray cameras: the Gas Slit Camera (GSC; Mihara et al. 2011; Sugizaki et al. 2011) for the 2−30 keV band and Solid-state Slit Camera (SSC; Tsunemi et al. 2010; Tomida et al. 2011) for the 0.5−12 keV band, using gas proportional counters and X-ray CCDs, respectively. Since the time resolution of the SSC (5.6 s) is too long to detect the pulsation of the Crab pulsar, we concentrate on the analysis of the GSC data in this paper.

The GSC scans almost all the sky every 92 minutes with a field of view (FoV) of 1.°5

(FWHM) by 160°. The effective area for any source is calculated according to the collimator transmission function of a triangular shape during each scan transit (Sugizaki et al. 2011; Morii et al. 2006; Morii, Sugimori & Kawai 2010). The spatial resolution of the GSC is approximately 1.°5 (FWHM). The time resolution of the GSC is 50 μs. We confirmed that the relative event time was stable within the standard deviation of 0.2 ms throughout the whole observation period. The absolute time assignment was also confirmed as accurate within the stability of the relative time, by comparing the main peak phase of the Crab pulsar obtained by the GSC with that of the RXTE PCA observation (Rots, Jahoda & Lyne 2004).

3. Analysis and Results

3.1. Pulse phase averaged flux of the Crab nebula

We examined the variation of the entire Crab nebula flux averaged over the pulse phase. We employed the same procedure to derive the Crab flux to that in the effective-area calibration described in Sugizaki et al. (2011). The source event data were extracted from the region of 1.°6 radius from the Crab nebula. The background level was estimated from the data for the adjacent source-free sky region within the annulus with the inner and outer radii of 1.°6 and 3.°2, respectively, where the region contaminated by the nearby bright source, namely A 0535+262, was excluded. We used the data of the four anodes (C0, C3, C4, and C5) among the total of six (C0−C5) for all the counters in this analysis because the other two were not calibrated well for the complex energy-PHA responses (Sugizaki et al. 2011). Figure 1 (top panel) shows the light curve obtained in the 4−10 keV band in 2.5-day time bins. Here, the binning boundaries were carefully chosen to divide the flare period (MJD 55457.5−55462.5) into two periods "A" and "B" at MJD 55460 (see figure 2 in Balbo et al. 2011). The flux for the entire flare period "A+B" and those for Periods A and B are shown in table 1.

The small fluctuations in the light curve are thought to be not intrinsic to the Crab nebula, but due to the systematic uncertainties in the GSC effective area calibration. To estimate the systematic uncertainty, we fitted the light curve with linear functions, the decline rate of which was either set free or fixed to that determined with the RXTE PCA light curve from MJD 54690 to 55435 in the 2−15 keV band (Wilson-Hodge et al. 2011). The obtained parameters of the model functions are shown in table 2, where they are denoted as "Average: linear (free)" and "Average: linear (fixed)", respectively. Assuming that the systematic uncertainty affects all the data bins uniformly and is proportional to the flux, we estimate the systematic uncertainty by calculating the modified reduced chi-squared $\chi^2_{\rm red} = \frac{1}{\rm DOF}\sum_i[(F_i - F_{\rm model}(t_i))^2]/[\sigma^2_{F_i} + (r_{\rm syst}F_i)^2]$ for a tentative systematic uncertainty ($r_{\rm syst}$). Here, F_i and σ_{F_i} are the flux and statistical error at the i-th time bin (t_i), respectively. $F_{\rm model}$ and DOF are the model function for the flux and the degree of freedom, respectively. We then estimated the systematic uncertainty of 1-σ level by searching for the $r_{\rm syst}$ to make the reduced chi-squared unity. The obtained systematic un-

certainties were 2% in both cases. On the other hand, the maximum deviation from the best-fit functions was 8% among 118 time bins in both cases. Since the latter deviation is statistically large in comparison with the former uncertainty, there are some peculiar bins which are subject to larger systematic uncertainty.

The flux variations observed during Periods A, B, and A+B are statistically consistent with the best fit linear model. We calculated the upper limits on the variation of the flux during the flare, expressed by the excess ratio (%) to the best-fit model functions (table 2). The statistical 90% confidence level upper limits during Period A+B are 1.0 and 0.8% for the two linear model functions. The values during Periods A and B are also shown in table 2.

To investigate the variability corresponding to the sub-flares observed by Fermi-LAT (Balbo et al. 2011), we made the 0.5-day binned light curve in the 4−10 keV band during the flare interval as shown in figure 2 (top panel). The deviation from the best-fit linear function "Average: linear (free)" of table 2 is not statistically significant with a reduced chi-squared of 1.13 for 12 degree of freedom (DOF).

3.2. Pulsed flux of the Crab pulsar deduced from sub-scan-duration data analysis

To measure the pulsed flux of the Crab pulsar, we analyzed the data by the following steps. Since the background rate within the FoV depends on the position in the detector, we extracted events based on the detector coordinate. We selected events within 5 mm from the position coincident with the Crab nebula along the anode wires, which corresponds to about 2° on the sky. We removed events from the scan period when the instantaneous effective area of a GSC camera was smaller than 1 cm^2. This is because the systematic uncertainty and the signal-to-background ratio worsen under this condition. The photon arrival times were corrected to the solar system barycenter by `mxbarycen`, the validity of which was confirmed by the timing calibration (Sugizaki et al. 2011). We chose the energy band of $4-10$ keV. The events with corrected times were folded in the pulse period of the Crab pulsar of the Jodrell Bank radio observatory (Lyne, Pritchard, & Smith 1993). We applied corrections of the effective area and exposure in this step.

The pulse profile during Period A+B is shown in figure 3, where the phase zero corresponds to that of the first main pulse in radio (Lyne, Pritchard, & Smith 1993). To compare it with the normal pulse profile of the Crab pulsar, we made a template pulse profile $T(\phi_i)$ ($i = 1$st, $\cdots$, N-th phase bin; $N = 64$ and ϕ is the pulse phase.) by averaging the profile from 2009 December 13 to 2010 January 11, in which the un-pulsed component was subtracted. We fit the pulse profile during the gamma-ray flare to a model $a \times T(\phi) + b$, where a and b represent the scale factor of the pulsed component relative to the template and the constant offset representing the background and the nebula component. The best-fit model is shown as the solid line in figure 3, where the reduced chi-squared of the fit is 1.34 for 62 DOF. We also performed the same analysis for the pulse profiles during Periods A and B. The reduced chi-squared of the

Table 1. Pulse phase averaged and pulsed fluxes of the Crab nebula in $4-10$ keV.

Flux*	Period A†	Period B‡	Period A+B§
Averaged	1.21 ± 0.02	1.23 ± 0.02	1.22 ± 0.01
Pulsed	0.13 ± 0.02	0.18 ± 0.02	0.16 ± 0.01

*photons cm^{-2} s^{-1} with 1-σ statistical error.

†MJD 55457.5−55460.0. ‡MJD 55460.0−55462.5.

§MJD 55457.5−55462.5

Table 2. Model parameters and upper limits on the variation of the flux of the Crab nebula in $4-10$ keV

Model		Average: linear* (free)	Average: linear* (fixed)	Pulsed: const
Parameters	Flux†	1.241(2)	1.242(1)	0.145(1)
	Slope†	$(-8.5 \pm 1.0) \times 10^{-5}$	-7.2×10^{-5}(fix)	—
Upper limits‡	Period A§	0.8%	0.6%	9.0%
	Period B§	2.4%	2.1%	37.3%
	Period A+B§	1.0%	0.8%	18.8%

*The linear function is $F(t) = F(t_{\rm mid})\,[1 + S \times (t - t_{\rm mid})]$, where $F(t)$, t, $t_{\rm mid}$ and S are the flux (photons cm^{-2} s^{-1}), time (day), mid-time (MJD 55312.5) and the slope (day^{-1}), respectively.

†At the mid-time with 1-σ statistical error.

‡Statistical 90% confidence level. §Same as table 1.

fits are 0.92 and 1.35 for 62 DOF in these periods. All the pulse profiles during Periods A, B and A+B are consistent with the template pulse profile within the 99% confidence limit. From the pulse profile fitting, we also obtained the pulsed flux by $a\sum_i T(\phi_i)/N$ [1], the results of which are shown in table 1. This method is free from background variation because the background variation only affects the offset parameter b.

We repeated the same analysis from 2009 November 1 to 2010 November 29 every 2.5 days to make the light curve of the pulsed flux in the 4−10 keV band [Figure 1 (bottom panel)] and fitted it by a constant. The reduced chi-squared of the fit is 1.27 for 104 DOF, meaning that there was no evidence of variability. The flux obtained is shown in table 2. The flux variations observed during Periods A, B, and A+B are statistically consistent with the best fit function. The statistical 90% confidence level upper limits on the variation of the pulsed fluxes for these periods are 9.0, 37.3, and 18.8%, respectively (table 2). The 0.5-day binned light curve of the pulsed flux around the flare period is shown in figure 2 (bottom panel). The variation from the best-fit constant function "Pulsed: const" of table 2 is not statistically significant with a reduced chi-squared of 1.44 for 12 DOF.

[1] Please note that the pulse profiles are not normalized to unity but have the unit of counts cm^{-2} s^{-1}. Therefore, this value becomes the pulsed flux.

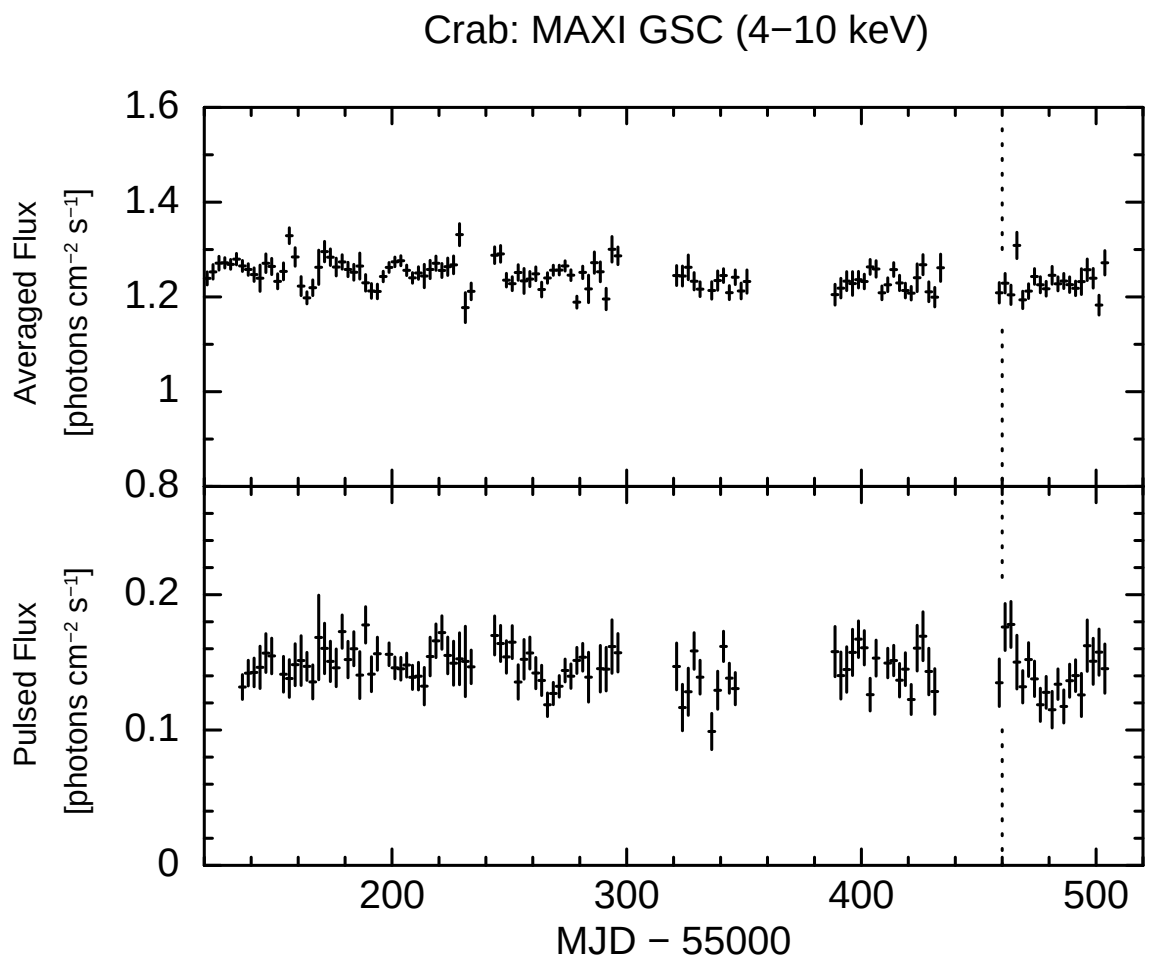

Fig. 1. GSC light curves of the pulse phase averaged flux (top panel) and pulsed flux (bottom panel) of the Crab nebula in the 4−10 keV band in 2.5-day time bins from 2009 October 16 to 2010 November 20 (MJD 55120−55520). The horizontal and vertical axes are shown in units of MJD minus 55000 (2009 June 18) and photons cm^{-2} s^{-1}, respectively. The vertical error bars correspond to 1-σ statistical errors. The time center (2010 September 21; MJD 55460.0) of the period of the GeV gamma-ray flare (MJD 55457.5−55462.5) is denoted by a vertical dotted line.

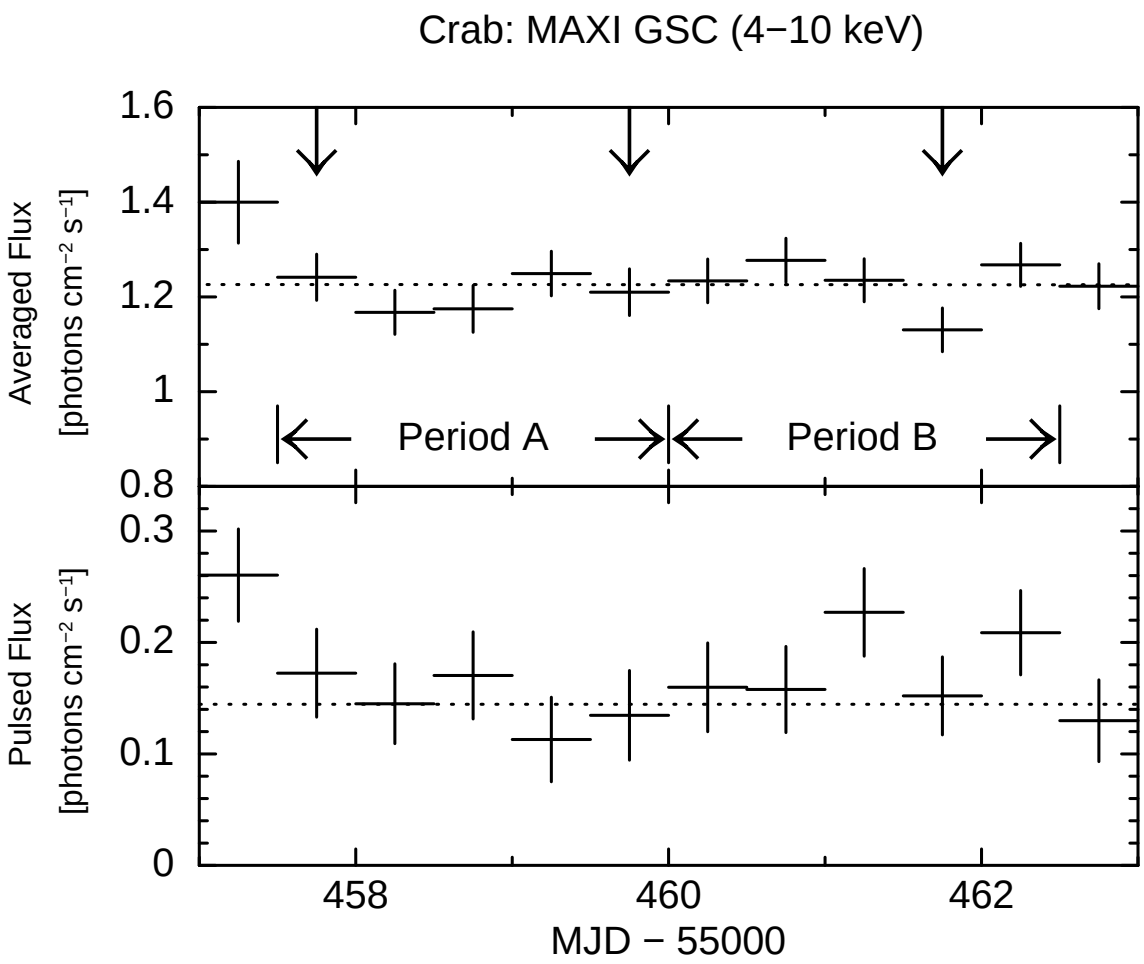

Fig. 2. Detailed light curve of figure 1 around the GeV gamma-ray flare from 2010 September 18 to 24 (MJD 55457−55463) in 0.5-day time bin. The horizontal and vertical axes are shown in the same units as figure 1. The vertical error bars correspond to 1-σ statistical errors. The peak times of the gamma-ray sub-flares (Balbo et al. 2011) are designated in three downward arrows. In the top and bottom panels, the dotted lines show the linear function "Average: linear (free)" and the constant value "Pulsed: const" with the best-fit parameters of table 2, respectively.

4. Conclusion

We report on the MAXI GSC observation of the Crab nebula during the GeV gamma-ray flare. We successfully detected the pulsation of the Crab pulsar during the simultaneous period, and conclude that there is no evidence for changes in the pulse profile, pulsed flux and pulse phase averaged flux during the gamma-ray flare. We obtained an upper limit on the variation of the pulse phase averaged flux of 1% at a 90% confidence limit of the statistical uncertainty from the best-fit linear function during the 5 day interval of the gamma-ray flare in the 4−10 keV band. During the same period in the same energy band, we also obtained an upper limit on the variation of the pulsed flux of 19% at a 90% confidence limit of statistical uncertainty from the mean level.

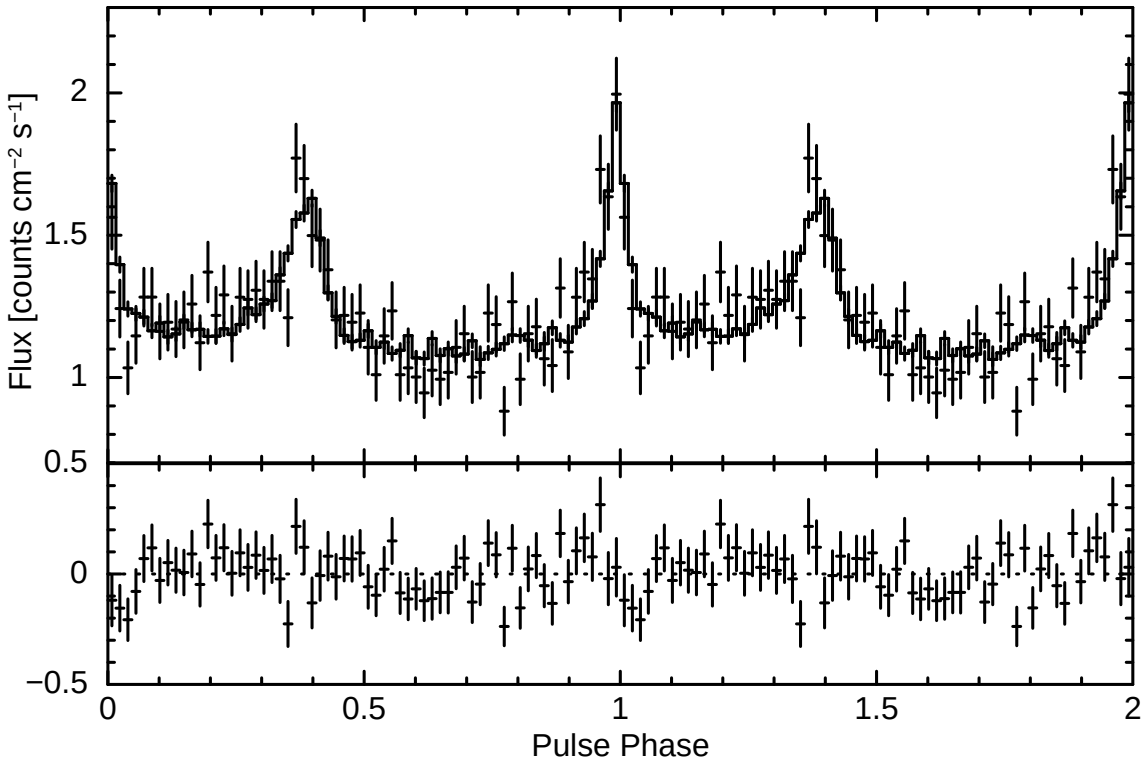

Fig. 3. Top panel: Pulse profile of the Crab pulsar in the 4−10 keV during the GeV gamma-ray flare for Period A+B (MJD 55457.5−55462.5) obtained by the GSC. The vertical axis is the flux shown in a unit of counts cm^{-2} s^{-1}. The horizontal axis is the pulse phase. The solid histogram is the template pulse profile with the best-fit parameters (see text). The bottom panel is the residual of the data from the best-fit model shown in the same unit with the top panel. In both panels, the vertical error bars correspond to 1-σ statistical errors. The same profiles are shown in two cycles.

The MAXI GSC simultaneous observation with the gamma-ray flare is uniquely important to constrain the origin of the flare, in contrast to the follow-up observations performed after the cease of the gamma-ray flare. The lack of changes on the pulsed component in the X-ray (this work), as well as those in radio (Espinoza et al. 2010), hard X-ray (Super-AGILE observation at the flare on 2007 shown in Tavani et al. (2011)) and gamma-ray bands (Tavani et al. 2011; Abdo et al. 2011), supports the nebular origin for the gamma-ray flare as proposed in several papers (Tavani et al. 2011; Abdo et al. 2011; Bednarek & Idec 2010; Yuan et al. 2010; Komissarov & Lyutikov 2010). In spite of the large flux increase of factor five in the GeV energy region (Abdo et al. 2011), we constrain a limit on the variation of the nebula flux in the X-ray band. This provides valuable information to construct theoretical models for the gamma-ray flare of the Crab nebula.

We are grateful to the members of the MAXI operation team. We acknowledge the use of the Crab ephemeris provided at the web site of the Jodrell Bank Centre for Astrophysics (Lyne, Pritchard, & Smith 1993). This research was partially supported by the Ministry

of Education, Culture, Sports, Science and Technology (MEXT), Grant-in-Aid No.19047001, 20041008, 20540230, 20244015 , 20540237, 21340043, 21740140, 22740120, and Global-COE from MEXT "The Next Generation of Physics, Spun from Universality and Emergence" and "Nanoscience and Quantum Physics."

References

Abdo, A. A., et al. 2011, Science, 331, 739

Aielli, G., et al. 2010, Astron. Telegram, 2921

Balbo, M., Walter, R., Ferrigno, C., & Bordas, P. 2011, A&A, 527, L4

Bednarek, W. & Idec, W. 2010, MNRAS, in the press (arXiv:1011.4176)

Buehler, R., et al. 2010, Astron. Telegram, 2861

Caraveo, P., et al. 2010, Astron. Telegram, 2903

Espinoza, C. M., Jordan, C., Stappers, B. W., Lyne, A. G., Weltevrede, P., Cognard, I., & Theureau, G., 2010, Astron. Telegram, 2889

Evangelista, Y., et al. 2010, Astron. Telegram, 2866

Ferrigno, C., Walter, R., Bozzo, E., & Bordas, P. 2010a, Astron. Telegram, 2856

Ferrigno, C., Tennant, A., Horns, D., Weisskopf, M. C., Neronov, A., Tavani, M., Costa, E., & Caraveo, P. 2010b, Astron. Telegram, 2994

Kanbach, G., Kruehler, T., Steiakaki, A., & Mignani, R. 2010, Astron. Telegram, 2867

Komissarov, S. S. & Lyutikov, M., 2010, MNRAS, in press (arXiv:1011.1800)

Heinke, C. O., 2010, Astron. Telegram, 2868

Horns, D., Tennant, A., Ferrigno, C., Weisskopf, M. C., Neronov, A., Tavani, M., Costa, E., & Caraveo, P. 2010, Astron. Telegram, 3058

Lyne, A. G., Pritchard, R. S., & Smith, F. G., 1993, MNRAS, 265, 1003. http://www.jb.man.ac.uk/research/pulsar/crab.html.

Mariotti, M., et al. 2010, Astron. Telegram, 2967

Markwardt, C. B., Barthelmy, S. D., & Baumgartner, W. H., 2010, Astron. Telegram, 2858

Matsuoka, M., et al. 2009, PASJ, 61, 999

Mihara, T., et al. 2011, PASJ, accepted (arXiv:1103.4224).

Morii, M., et al. 2006, Proc. of SPIE 6266, 6263U

Morii, M., Sugimori, K., & Kawai, N., 2010, Physica E: Low-dimensional Systems and Nanostructures, 43, 692.

Ong, R. A., et al. 2010, Astron. Telegram, 2968

Yuan, Q., Yin, P.-F., Wu, X.-F., Bi, X.-J., Liu, S., & Zhang, B., 2011, ApJ, 730, L15

Rots, A. H., Jahoda, K & Lyne, A. G., 2004, ApJ, 605, L129

Shaposhnikov, N., Jahoda, K., Swank, J., Strohmayer, T., Markwardt, C., & Weisskopf, M., 2010, Astron. Telegram, 2872

Sugizaki, M., et al. 2011, PASJ, accepted (arXiv:1102.0891).

Tavani, M., et al. 2010, Astron. Telegram, 2855

Tavani, M., et al. 2011, Science, 331, 6018, 736

Tennant, A., et al. 2010, Astron. Telegram, 2882
Tomida, H., et al. 2011, PASJ, accepted (arXiv:1101.3651).
Tsunemi, H., Tomida, H., Katayama, H., Kimura, M., Daikyuji, A., Miyaguchi, K., Maeda, K., & the MAXI team, 2010, PASJ, 62, 1371
Wilson-Hodge, C. A., et al. 2011, ApJL, 727, L40